VECTOR-BORNE AND ZOONOTIC DISEASES
Volume 20, Number 3, 2020
© Mary Ann Liebert, Inc.
DOI: 10.1089/vbz.2019.2495

Molecular Characterization of Hamster-Adapted Yellow Fever Virus

Monica A. McArthur,[1,2] Shuliu L. Zhang,[3,†] Li Li,[3,4] Robert B. Tesh,[3] and Alan D.T. Barrett[3,4]

Abstract

We previously reported two hamster models for viscerotropic yellow fever virus (YFV) infection: one using a YFV strain (Jiménez), isolated from a fatal human case in Panama in 1974, and the other using the prototype YFV strain (Asibi). Asibi hamster passage 7 (P7) was associated with accumulation of seven amino acid substitutions, including five in the envelope protein. In this study we report the genome sequences of the hamster Jiménez P0 and P10 viruses in which we identified only two amino acid substitutions during passage, one each in the nonstructural proteins NS3 and NS5, indicating a role for the nonstructural proteins in increased YFV viscerotropism in the Jiménez hamster model. Thus, there are multiple molecular mechanisms involved in viscerotropism of YFV in the hamster model. Neither Asibi P7 nor Jiménez P10 viruses were viscerotropic in mice or guinea pigs. Thus, the hamster viscerotropic phenotype did not translate to other laboratory rodent species.

Keywords: Yellow fever virus, viscerotropism, hamster model, viral pathogenesis

Introduction

YELLOW FEVER VIRUS (YFV) is an important re-emerging human pathogen that still causes significant morbidity and mortality in tropical regions of Africa and South America. It frequently causes a viscerotropic infection leading to hemorrhagic fever and death in humans and nonhuman primates (Monath and Vasconcelos 2015, Couto-Lima et al. 2017, Hamrick et al. 2017, Lilay et al. 2017, Gomez et al. 2018, Shearer et al. 2018). YFV is the prototypic member of the genus *Flavivirus*, family Flaviviridae. The flavivirus genome is a positive-sense single stranded RNA molecule ~11 kb in length (Rice et al. 1985). The genome contains a single open reading frame (ORF) flanked by 5′ and 3′ nontranslated regions (NTR). The ORF encodes a polyprotein of ~3400 amino acids that is co- and post-translationally cleaved to generate three structural proteins, core (C), membrane (M), and envelope (E) as well as seven nonstructural genes, NS1, NS2A, NS2B, NS3, NS4A, NS4B, and NS5.

We previously reported two hamster models for viscerotropic YFV infection. The first using YFV strain Jiménez, isolated from a fatal human case in Panama in 1974 (Tesh et al. 2001, Xiao et al. 2001, Sbrana et al. 2006), and the second using the prototype YFV strain (Asibi), isolated from a nonfatal human case in Ghana in 1927 (McArthur et al. 2003, 2005). The nonhamster-passaged Jiménez virus (Jiménez P0) caused a nonfatal infection in Syrian golden hamsters (*Mesocricetus auratus*) with moderate viremia. However, after 10 serial hamster passages (Jiménez P10), the virus produced higher levels of viremia, histopathologic and biochemical changes consistent with yellow fever, and a mortality rate of 20–80%, depending upon the age (adult vs. 3–4 weeks) of the hamsters (Supplementary Table S1) (Tesh et al. 2001, Xiao et al. 2001, Sbrana et al. 2006). Similarly, the nonhamster-passaged Asibi strain (Asibi P0) produced no clinical illness and only moderate viremia in 3- to 4-week-old hamsters; but after seven serial hamster passages, the virus (Asibi P7) was 100% lethal in the hamster model and was associated with high viremia and histopathologic changes consistent with viscerotropic YFV infection (Supplementary Table S1) (McArthur et al. 2003). Comparison of the full genomic sequences of YFV Asibi P0 and P7 identified 14 nucleotide differences encoding 7 aminos acid substitutions,

[1]Center for Vaccine Development and Global Health, University of Maryland School of Medicine, Baltimore, Maryland.
[2]Department of Pediatrics, University of Maryland School of Medicine, Baltimore, Maryland.
[3]Department of Pathology, University of Texas Medical Branch, Galveston, Texas.
[4]Sealy Institute for Vaccine Sciences, University of Texas Medical Branch, Galveston, Texas.
[†]Deceased.

of which 5 were in the E protein (McArthur et al. 2003). Klitting et al. (2018) further identified a T154A mutation in the E protein (adjacent to the E-D 155A mutation reported by our group previously) as partially responsible for the viscerotropic phenotype in hamsters.

Extensive characterization of the clinical parameters and histopathology associated with Jiménez P0 and P10 viruses have been reported (Tesh et al. 2001, Xiao et al. 2001, Sbrana et al. 2006). This animal model has also been used to test antiviral treatments against YFV infection (Sbrana et al. 2004, Julander et al. 2009, 2014, Julander 2016). However, there have been no reports of the molecular characterization of these two Jiménez viruses. In this study we describe the full-length sequence of the parental Jiménez P0 and its hamster-passaged derivative Jiménez P10, as well as the phenotype of hamster-passaged YFV in other rodent species.

Materials and Methods

Viruses

All viruses were received from the World Reference Center for Emerging Viruses and Arboviruses, University of Texas Medical Branch, and were given one additional passage in Vero cells to produce a working stock.

Cell culture

Viruses were cultured in Vero cells (green monkey kidney cell line) for 6–10 days. Before infection, Vero cells were split and allowed to grow for a minimum of 24 h (to a confluency of ~75–80%) before infection. Cells were washed once with phosphate-buffered saline and 100 μL of virus was added to the culture flask. The flask was incubated at room temperature for 30–45 min after which minimal essential media (MEM) supplemented with 2% bovine growth serum, 0.3% L-glutamine (Gibco-BRL, Gaithersburg, MD), 1% nonessential amino acids (Sigma, Saint Louis, MO), and 1% penicillin/streptomycin (Gibco-BRL) was added. Infected cultures were maintained at 37°C with 5% CO_2 until cytopathic effects (cpe) were evident.

Virus was harvested when the cultures began to show cpe. All virus cultures were maintained in BSL3 facilities. Viral titers were measured by 50% tissue culture infectious dose ($TCID_{50}$). In brief, virus was serially diluted in 96 well plates (each virus was titrated in triplicate when possible). After virus dilution, 100 μL of Vero cells was added to each well. The edges of the plates were taped to prevent drying and placed at 37°C for 7–10 days. The highest dilution at which cpe were observed was recorded for each column, and the Reed–Meunch method was used to calculate the $TCID_{50}$.

Reed–Meunch method. The proportionate distance between the dilution that causes cpe in >50% of the infected wells and the dilution that causes cpe in <50% of the infected wells was calculated.

$$\frac{(\%\ \text{positive above } 50\%) - 50\%}{(\%\ \text{positive above } 50\%) - (\%\ \text{positive below } 50\%)}.$$

The 50% end-point is now calculated. This is the $\log_{10}$ ID_{50} (log dilution >50%) + (proportionate distance × $\log_{10}$ dilution factor). Finally, the titer is converted into $\log_{10}$ $TCID_{50}$/mL.

Virus RNA isolation, amplification, and sequencing

Virus RNA was isolated using the Qiagen RNA extraction kit, and resuspended in 80 μL of HPLC grade water followed by RT-PCR using a set of overlapping primer pairs (Supplementary Table S2).

PCR fragments were cloned into the pGEM vector (Invitrogen) and amplified in *Escherichia coli* DH5α competent cells. Forward and reverse sequences were obtained from each fragment, and two to three clones of each fragment were sequenced to obtain a consensus sequence. Sequencing was performed in the UTMB Protein Chemistry Core Laboratory. Supplementary Table S2 contains a list of primers used for sequencing. Genomic sequences were assembled and aligned using the Vector NTI software package (InforMax).

Animals

Female outbred guinea pigs, 2–3 weeks of age, and female NIH Swiss mice, 3–4 weeks of age (Harlan Bioproducts; Indianapolis IN), were inoculated intraperitoneally (ip) with 100 μL of YFV stock (Asibi P0, Asisbi P7, Jiménez P0 or Jiménez P10) containing 7 $\log_{10}$ $TCID_{50}$. On days 3 and 6 postinfection (pi), two animals from each group were exsanguinated by cardiac puncture, and liver, spleen, and brain were harvested at necropsy. Animals were anesthetized with halothane before procedures. Six animals from each experimental group were also observed until 14 days pi for outcome. IACUC approval number 93-07-048.

Neuroinvasiveness in 8-day-old mice

Untimed pregnant mice in late gestation were obtained from Harlan Bioproducts. Litters were inoculated ip with 100 μL of serially diluted virus to calculate the 50% lethal dose (LD_{50}). LD_{50} was calculated by the Reed– Muench method (Reed and Muench 1938).

Histopathology

Samples of liver, spleen, and brain from infected animals were fixed in 10% formalin, followed by paraffin embedding, sectioning, and staining with hematoxylin and eosin as described (Xiao et al. 2001) in the UTMB Histopathology Core Laboratory. Slides were blinded and evaluated for microscopic changes consistent with YFV infection.

Statistical analyses

Average survival times (ASTs) were compared using Mann–Whitney (GraphPad Prism 6.0, San Diego, CA).

Results

Sequence of the full-length Jiménez P0 and P10 genomes

The full-length genome of Jiménez P0 virus was 10,794 nucleotides in length with a single ORF of 10,233 nucleotides (3411 amino acids). The Jiménez P0 virus and its hamster-passaged derivative, Jiménez P10, differed by only five nucleotides encoding two deduced amino acid substitutions. There were no nucleotide changes located within the 5′ or 3′ NTR. The nucleotide changes in the Jiménez P10

virus were located at genome positions 1237, 2755, 4767, 6358, and 7646. Nucleotides 6358 and 7646 were nonsynonymous and encoded amino acid substitutions within the nonstructural proteins, NS3-R66K and NS5-N4D, respectively (Table 1).

The location of amino acid 66 of the NS3 N-terminal serine protease protein was modeled on the crystallographic structure of the DENV2 (dengue virus 2) serine protease protein using the SWISS-PDB program (Murthy et al. 1999), showing that residue 66 is distant from the catalytic triad (Fig. 1).

Residue 4 of NS5 (N→D in Jiménez P10) is located upstream of the putative 5′methyl-transferase domain, near the NS4B/NS5 cleavage site.

The Jiménez P0 virus (South American genotype I) (Auguste et al. 2010) differed from Asibi P0 (West African genotype II) (Beck et al. 2013) at 15 amino acid positions within the E protein; however, only 1 of these differences (residue 331) is shared with hamster viscerotropic Asibi P7 virus (Fig. 2).

Viscerotropism in other rodent models

Since the Asibi and Jiménez YFV strains accumulated different substitutions after serial passage in hamster liver, we investigated whether the viscerotropism (defined as clinically detectable signs of YFV infection, evidence of viremia, and/or histopathological lesions consistent with YFV infection) observed in the hamster model translated to other rodent species.

All of the guinea pigs inoculated by the ip route with the hamster viscerotropic (Asibi P7 and Jiménez P10) and nonhamster viscerotropic strains (Asibi P0 and Jiménez P0) of YFV survived and showed no clinical signs of illness throughout the course of these studies. Viremia was not detectable upon assay in Vero cells by $TCID_{50}$ in any of the animals on either day 3 or 6 pi. Similarly, virus was not detected in liver homogenates assayed by $TCID_{50}$, nor was it possible to amplify viral RNA from these samples. There were no histopathological changes in any tissues.

After ip inoculation of 3- to 4-week-old NIH Swiss mice with Asibi P0, Asibi P7, Jiménez P0, or Jiménez P10, there was no mortality in any group. During the 14-day observation period, none of the mice displayed clinical signs of illness compatible with YFV infection. Virus was not detected in the sera upon assay in Vero cells by $TCID_{50}$. No attempt was made to harvest virus from tissues as there was no detectable viremia and no evidence of histopathologic changes consistent with YFV infection.

Table 1. Nucleotide and Deduced Amino Acid Changes Between Jimenez P0 and P10 Yellow Fever Virus Strains

Nucleotide	*Jiménez P0*	*Jiménez P10*	*Amino acid*	*Jiménez P0*	*Jiménez P10*
1237	G	A			
2755	A	G			
4767	G	A			
6358	G	U	NS3-66	R	K
7646	A	G	NS5-4	N	D

Neuroinvasiveness in suckling mice

The well-characterized mouse neuroinvasive model of YFV infection using 8-day-old NIH Swiss mice (Wang et al. 1995) was used to determine whether the hamster-adapted viruses had any modification to their mouse neuroinvasive phenotype. Jiménez P0 stock had an LD_{50} of 1.0 ± 0.2 $\log_{10}$ $TCID_{50}$ with an AST of 11.7 ± 0.7 days, whereas Jiménez P10 had an LD_{50} of 0.8 ± 0.6 $\log_{10}$ $TCID_{50}$ and AST of 11.8 ± 1.9. There was no statistically significant difference between these values ($p > 0.05$, Mann–Whitney). The French neurotropic vaccine (FNV) strain, which is highly neuroinvasive in mice (Wang et al. 1995) but does not cause viscerotropic or neurotropic disease in hamsters, was used as a control. FNV had an LD_{50} of 1.3 ± 0.3 $\log_{10}$ $TCID_{50}$ and an AST of 9.3 ± 0.0, and was not significantly different from the values obtained for Jiménez P0 and Jiménez P10. Although the LD_{50} of Asibi P0 and Asibi P7 was considerably higher than those of the two Jiménez viruses (2.6 ± 1.2 $\log_{10}$ $TCID_{50}$ and 3.5 ± 0.3 $\log_{10}$ $TCID_{50}$, respectively), there was no statistically significant difference between the nonhamster viscerotropic Asibi P0 and the hamster viscerotropic Asibi P7 ($p > 0.05$, Mann–Whitney). Nor was there a statistically significant difference in AST between Asibi P0 and Asibi P7 viruses (10.7 ± 1.0 and 12.0 ± 1.0 days, respectively, $p > 0.05$, Mann–Whitney).

Discussion

This study characterized the genomes and rodent phenotypes of hamster viscerotropic and nonhamster viscerotropic YFV. Comparison of the Jiménez P0 and Jiménez P10 viruses

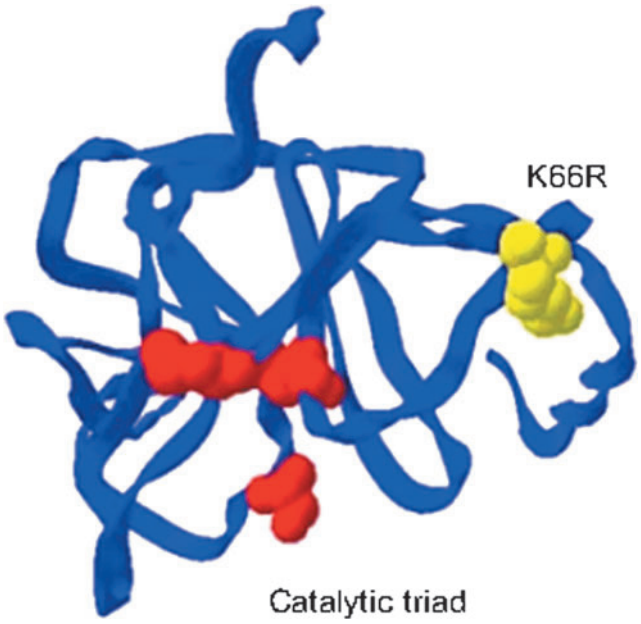

FIG. 1. Model of the YFV NS3 protease. The YFV NS3 was modeled on the crystallographic structure of DENV2 NS3 protease (Murthy et al. 2000) with SWISS-PDB. The catalytic triad is indicated in *red* and the location of the NS3-66 residue in *yellow*. DENV2, dengue virus 2; YFV, yellow fever virus.

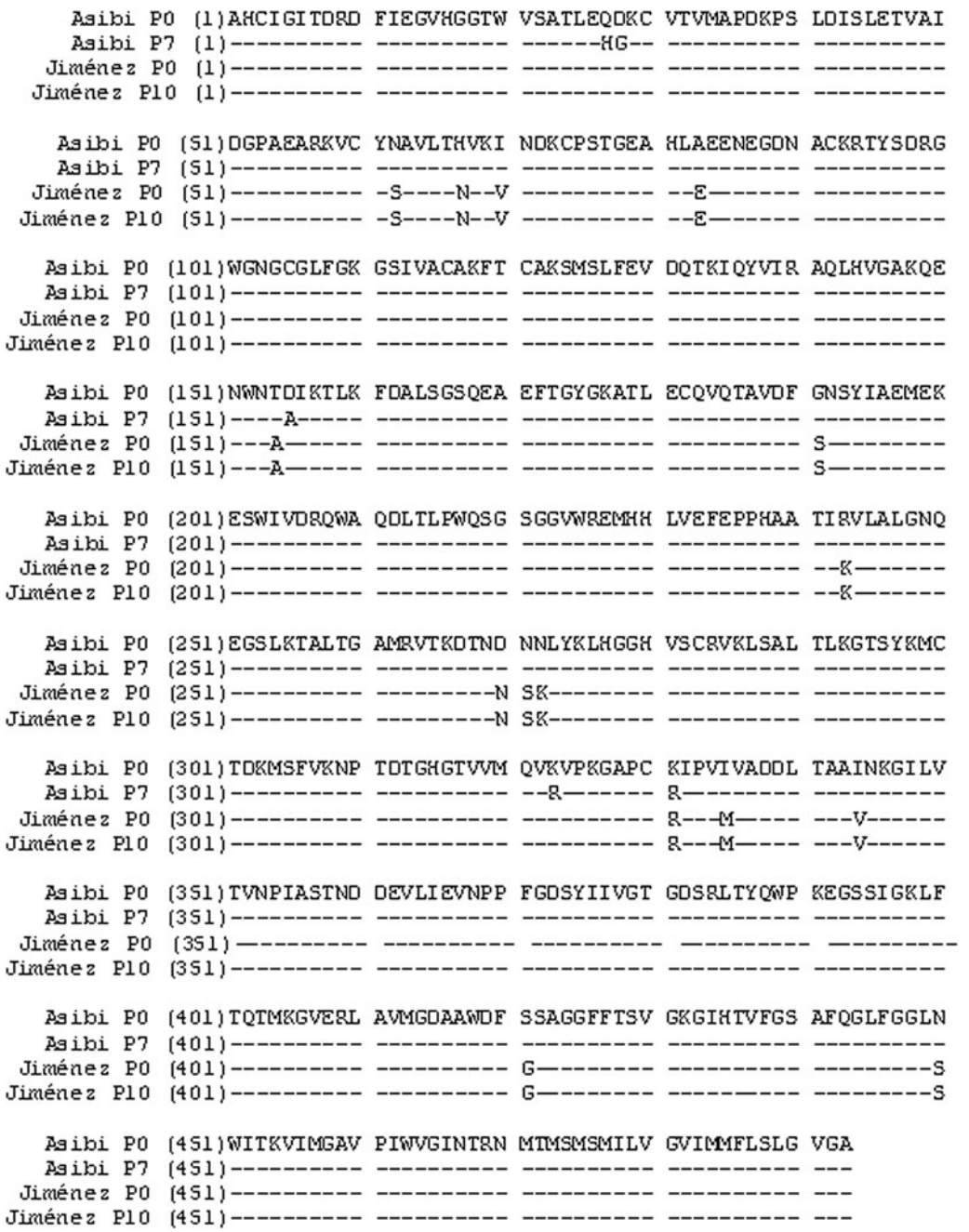

FIG. 2. Alignment of the E protein deduced amino acid sequences. The deduced amino acid sequences of Asibi P0, Asibi P7, Jiménez P0, and Jiménez P10 YFV strains are shown demonstrating amino acid differences among these viruses.

identified amino acid changes within the nonstructural proteins (NS3 and NS5). Unlike previous studies with the hamster viscerotropic Asibi P7, which implicated the E protein as a major determinant of viscerotropism (McArthur et al. 2003, 2005, Klitting et al. 2018), these studies indicate a possible role for nonstructural proteins in viscerotropism. Both NS3 and NS5 are found in the flavivirus replication complex (RC) and mutations in these proteins have been shown to alter virus replication (Lindenbach and Rice 2003). The NS3 protein contains both serine protease and helicase activities (Wengler 1991, Zhang et al. 1992, Pugachev et al. 1993, Chen et al. 1997, Cui et al. 1998, Valle and Falgout 1998) with residue 66 located within the protease domain. Furthermore, examination of the structure suggests that this residue may not play a direct role in protease activity. NS5 has multiple enzymatic functions including 5′methyltransferase and RNA-dependent RNA polymerase activities encoded by different domains (Rice et al. 1985, Koonin 1993, Tan et al. 1996, Ackermann and Padmanabhan 2001, Guyatt et al. 2001, Egloff et al. 2002). Residue 4 of NS5 is highly conserved among YFV strains; however, it is not believed to play a major role in cleavage at this site (Chambers et al. 1993). Given the differences in deduced amino acid changes between Asibi P0 and P7 ($n = 7$) compared with Jiménez P0

and P10 ($n=2$), there are likely multiple molecular mechanisms for viscerotropism in the hamster model.

Although previous studies, using the Asibi strain of YFV, have focused on the importance of the E protein in viscerotropism and proposed that alterations in recognition of and/or binding with host cell proteins are at least partially responsible for increased viscerotropism in the hamster model (McArthur et al. 2003), the lack of deduced amino acid substitutions in the E protein of the Jiménez P10 virus suggests that alteration in host cell recognition and/or binding is not a requirement for increased viscerotropism in the hamster model. It is, therefore, likely that different molecular mechanisms of hamster viscerotropism are involved in these two systems. Specifically, alterations in the RC of Jiménez P10 might allow increased viral replication within hamster hepatocytes and/or other target cells, leading to higher levels of viremia and clinical manifestations of YFV infection.

In addition to the deduced amino acid changes identified after hamster passage, there were several synonymous nucleotide changes. It is also possible that these silent mutations play a role in viscerotropism. It has been demonstrated that codon usage biases may alter translation leading to changes in replication efficiency (Di Paola et al. 2018). Thus, silent mutations may contribute to the differences in viscerotropism of passaged viruses in the hamster as well as the lack of viscerotropism in other rodent models.

We further investigated the phenotype developed by serial passage of YFV in hamsters in other rodent species and did not identify evidence of viscerotropism in either guinea pigs or mice. These data imply that the acquisition of viscerotropism is determined by different genetic factors in different hosts. This result was not unexpected, as there is a precedent for this observation in the mouse model of neurotropism (Wang et al. 1995). YFV is neurotropic in mice, and its passage in mice results in increased neurotropism (not viscerotropism) in the mouse model (*i.e.,* FNV). However, the increased neurotropism of mouse-adapted strains is not observed in other rodent species (Wang et al. 1995). Furthermore, guinea pigs have previously been shown to be resistant to YFV (Strode 1951). These results are consistent with the hypothesis that different nucleotides/amino acids encode the molecular determinants of neuroinvasiveness and viscerotropism in rodents.

Conclusions

In conclusion, the markedly different genetic backgrounds of the West African Asibi and South American Jiménez parental strains of YFV provided an ideal model in which to test the hypothesis that similar molecular mechanisms were associated with adaptation to the hamster model. These studies demonstrate that two hamster adaptation processes can result in similar viscerotropic phenotypes that can be encoded by multiple molecular mechanisms of adaptation. Further studies using YFV infectious clones may provide additional information regarding the relative contributions of these mutations on viscerotropism.

Acknowledgment

The authors thank the World Reference Center for Emerging Viruses and Arboviruses for provision of the YFV stocks.

Author Disclosure Statement

No competing financial interests exist.

Funding Information

Funding was received from the National Institutes of Health T32 AI7526, F31 AI54319 and NO1 AI30027.

Supplementary Material

Supplementary Table S1
Supplementary Table S2

References

Ackermann M, Padmanabhan R. De novo synthesis of RNA by the dengue virus RNA-dependent RNA polymerase exhibits temperature dependence at the initiation but not elongation phase. J Biol Chem 2001; 276:39926–39937.

Auguste AJ, Lemey P, Pybus OG, Suchard, et al. Yellow fever virus maintenance in Trinidad and its dispersal throughout the Americas. J Virol 2010; 84:9967–9977.

Beck A, Guzman H, Li L, Ellis B, et al. Phylogeographic reconstruction of African yellow fever virus isolates indicates recent simultaneous dispersal into east and west Africa. PLoS Negl Trop Dis 2013; 7:e1910.

Chambers TJ, Nestorowicz A, Amberg SM, Rice CM. Mutagenesis of the yellow fever virus NS2B protein: Effects on proteolytic processing, NS2B-NS3 complex formation, and viral replication. J Virol 1993; 67:6797–6807.

Chen Y, Maguire T, Hileman RE, Fromm JR, et al. Dengue virus infectivity depends on envelope protein binding to target cell heparan sulfate. Nat Med 1997; 3:866–871.

Couto-Lima D, Madec Y, Bersot MI, Campos SS, et al. Potential risk of re-emergence of urban transmission of Yellow Fever virus in Brazil facilitated by competent Aedes populations. Sci Rep 2017; 7:4848.

Cui T, Sugrue RJ, Xu Q, Lee, AKW, et al. Recombinant dengue virus type 1 NS3 protein exhibits specific viral RNA binding and NTPase activity regulated by the NS5 protein. Virology 1998; 246:409–417.

Di Paola N, Freire CCM, Zanotto PMA. Does adaptation to vertebrate codon usage relate to flavivirus emergence potential? PLoS One 2018; 13:e0191652.

Egloff MP, Benarroch D, Selisko B, Romette JL, et al. An RNA cap (nucleoside-2'-O-)-methyltransferase in the flavivirus RNA polymerase NS5: Crystal structure and functional characterization. EMBO J 2002; 21:2757–2768.

Gomez MM., Abreu FVS, Santos A, Mello IS, et al. Genomic and structural features of the yellow fever virus from the 2016–2017 Brazilian outbreak. J Gen Virol 2018; 99:536–548.

Guyatt KJ, Westaway EG, Khromykh AA. Expression and purification of enzymatically active recombinant RNA-dependent RNA polymerase (NS5) of the flavivirus Kunjin. J Virol Methods 2001; 92:37–44.

Hamrick PN, Aldighieri S, Machado G, Leonel DG, et al. Geographic patterns and environmental factors associated with human yellow fever presence in the Americas. PLoS Negl Trop Dis 2017; 11:e0005897.

Julander JG. Animal models of yellow fever and their application in clinical research. Curr Opin Virol 2016; 18:64–69.

Julander JG, Bantia S, Taubenheim BR, Minning DM, et al. BCX4430, a novel nucleoside analog, effectively treats yellow fever in a Hamster model. Antimicrob Agents Chemother 2014; 58:6607–6614.

Julander JG, Shafer K, Smee DF, Morrey JD, et al. Activity of T-705 in a hamster model of yellow fever virus infection in comparison with that of a chemically related compound, T-1106. Antimicrob Agents Chemother 2009; 53:202–209.

Klitting R, Roth L, Rey FA, De Lamballerie X. Molecular determinants of Yellow Fever Virus pathogenicity in Syrian Golden Hamsters: One mutation away from virulence. Emerg Microbes Infect 2018; 7:51.

Koonin EV. Computer-assisted identification of a putative methyltransferase domain in NS5 protein of flaviviruses and lambda 2 protein of reovirus. J Gen Virol 1993; 74(Pt 4):733–740.

Lilay A, Asamene N, Bekele A, Mengesha M, et al. Reemergence of yellow fever in Ethiopia after 50 years, 2013: Epidemiological and entomological investigations. BMC Infect Dis 2017; 17:343.

Lindenbach BD, Rice CM. Molecular biology of flaviviruses. Adv Virus Res 2003; 59:23–61.

Mcarthur MA, Suderman MT, Mutebi JP, Xiao SY, et al. Molecular characterization of a hamster viscerotropic strain of yellow fever virus. J Virol 2003; 77:1462–1468.

Mcarthur MA, Xiao SY, Barrett AD. Phenotypic and molecular characterization of a non-lethal, hamster-viscerotropic strain of yellow fever virus. Virus Res 2005; 110:65–71.

Monath TP, Vasconcelos PF. Yellow fever. J Clin Virol 2015; 64:160–173.

Murthy K, Clum S, Padmanabhan R. Dengue virus NS3 serine protease: Crystal structure and insights into interaction of the active site with substrates by molecular modeling and structural analysis of mutational effects. J Biol Chem 1999; 274: 5573–5580.

Murthy K, Judge K, Delucas L, Padmanabhan R. Crystal structure of dengue virus NS3 protease in conplex with a Bowman-Birk inhibitor: Implications for flavivirus polyprotein processing and drug design. J Mol Biol 2000; 301: 759–767.

Pugachev KV, Nomokonova NU, Dobrikova EY, Wolf YL. Site-directed mutagenesis of the tick-borne encephalitis virus NS3 gene reveals the putative serine protease domain of the NS3 protein. FEBS Lett 1993; 328:115–118.

Reed LJ, Muench H. A simple method of estimating fifty percent endpoints. Am J Hyg 1938; 27:493–497.

Rice CM, Lenches EM, Eddy SR, Shin SJ, et al. Nucleotide sequence of yellow fever virus: Implications for flavivirus gene expression and evolution. Science 1985; 229:726–733.

Sbrana E, Xiao SY, Guzman H, Ye M, et al. Efficacy of postexposure treatment of yellow fever with ribavirin in a hamster model of the disease. Am J Trop Med Hyg 2004; 71:306–312.

Sbrana E, Xiao SY, Popov VL, Newman PC. et al. Experimental yellow fever virus infection in the golden hamster (*Mesocricetus auratus*) III. Clinical laboratory values. Am J Trop Med Hyg 2006; 74:1084–1089.

Shearer, FM, Longbottom J, Browne AJ, Pigott DM, et al. Existing and potential infection risk zones of yellow fever worldwide: A modelling analysis. Lancet Glob Health 2018; 6: e270–e278.

Strode GK. *Yellow Fever.* New York: McGraw-Hill Book Company, Inc., 1951.

Tan BH, Fu J, Sugrue RJ, Yap EH, et al. Recombinant dengue type 1 virus NS5 protein expressed in *Escherichia coli* exhibits RNA-dependent RNA polymerase activity. Virology 1996; 216:317–325.

Tesh RB, Guzman H, Da Rosa AP, Vasconcelos PF, et al. Experimental yellow fever virus infection in the Golden Hamster (*Mesocricetus auratus*). I. Virologic, biochemical, and immunologic studies. J Infect Dis 2001; 183:1431–1436.

Valle RPC, Falgout B. Mutagenesis of the NS3 protease of dengue virus type 2. J Virol 1998; 72:624–632.

Wang E, Ryman KD, Jennings AD, Wood DJ, et al. Comparison of the genomes of the wild-type French viscerotropic strain of yellow fever virus with its vaccine derivative French neurotropic vaccine. J Gen Virol 1995; 76(Pt 11):2749–2755.

Wengler G. The carboxy-terminal part of the NS 3 protein of the West Nile flavivirus can be isolated as a soluble protein after proteolytic cleavage and represents an RNA-stimulated NTPase. Virology 1991; 184:707–715.

Xiao SY, Zhang H, Guzman H, Tesh RB. Experimental yellow fever virus infection in the Golden hamster (*Mesocricetus auratus*). II. Pathology. J Infect Dis 2001; 183:1437–1444.

Zhang L, Mohan PM, Padmanabhan R. Processing and localization of Dengue virus type 2 polyprotein precursor NS3-NS4A-NS4B-NS5. J Virol 1992; 66:7549–7554.

Address correspondence to:
Monica A. McArthur
Center for Vaccine Development and Global Health
University of Maryland School of Medicine
485 West Baltimore Room 480
Baltimore, MD 21201

E-mail: mmcarthu@som.umaryland.edu

Alan D.T. Barrett
Sealy Institute for Vaccine Sciences
University of Texas Medical Branch
301 University Boulevard
Galveston, TX 77555-0436

E-mail: abarrett@utmb.edu